β-Caryophyllene Protects Male Fertility and Testicular Function Against Paclitaxel-Induced Damage in a Murine Model

Peramaiyan Rajendran

prajendran@kfu.edu.sa

King Faisal University

Ramya Sekar

Meenakshi Ammal Dental College & Hospital, Meenakshi Academy of Higher Education and Research (Deemed to be University)

Rebai Ben Ammar

King Faisal University

Gmal K Behket

King Faisal University

Najla K. Al Abdulsalam

King Faisal University

Sayeed Al-Ramadan

Veterinary College of Medicine, King Faisal University

Dayashankar Praveena

Government Medical College

Enas M Ali

King Faisal University

Basem M Abdallah

King Faisal University

Research Article

Keywords: Paclitaxel, β-Caryophyllene, Testicular toxicity, Oxidative stress, p-AMPK/SIRT3/Nrf2 signaling

Posted Date: February 18th, 2026

DOI: https://doi.org/10.21203/rs.3.rs-8844033/v1

Additional Declarations: No competing interests reported.

Abstract

β-Caryophyllene (BCP) is a naturally occurring dietary sesquiterpene found in various edible plants and spices, such as clove, black pepper, and cinnamon, and is noted for its strong antioxidant and anti-inflammatory effects. Nevertheless, its preventive function against chemotherapy-induced male reproductive damage has not been sufficiently investigated. This study examined the functional dietary potential of BCP in alleviating paclitaxel (PTX)-induced testicular damage and explained its underlying molecular mechanisms. Five groups of male rodents were randomly assigned: control, BCP alone, PTX, PTX + BCP (low dose), and PTX + BCP (high dose). We assessed oxidative stress markers in the testicles and used Western blotting to examine at the protein levels of p-AMPK, SIRT3, Nrf2, and markers of apoptosis. Histopathological changes, collagen accumulation, and apoptotic cell death were assessed via hematoxylin–eosin, Masson's trichrome, and TUNEL tests, respectively. PTX administration significantly altered testicular homeostasis, as indicated by inhibited p-AMPK/SIRT3/Nrf2 signaling, reduced antioxidant enzyme activities, heightened lipid peroxidation and oxidative DNA damage, increased pro-inflammatory cytokines, and augmented apoptosis. These molecular alterations were associated with significant histological deterioration, excessive collagen accumulation, diminished serum testosterone concentrations, decreased testicular coefficient, and compromised sperm quality. Notably, BCP co-treatment dose-dependently restored antioxidant capacity, reactivated p-AMPK/SIRT3/Nrf2 signaling, suppressed inflammatory and apoptotic responses, and protected testicular architecture and reproductive function. BCP alone did not cause any bad effects. Conclusion: β-caryophyllene, a bioactive dietary ingredient, demonstrates substantial protective benefits against PTX-induced testicular toxicity through the activation of the p-AMPK/SIRT3/Nrf2 pathway. These results underscore BCP as a viable functional food-derived adjuvant for ameliorating chemotherapy-induced male reproductive failure.

1. Introduction

β-Caryophyllene (BCP) is a naturally occurring bicyclic sesquiterpene found in commonly consumed foods and spices, including black pepper (*Piper nigrum*), cloves (*Syzygium aromaticum*), cinnamon (*Cinnamomum spp.*), oregano (*Origanum vulgare*), basil (*Ocimum basilicum*), rosemary (*Rosmarinus officinalis*), thyme, and bay leaves, thus constituting a regular element of the human diet (1-3). Despite BCP lacking caloric energy and vital nutrients like vitamins or minerals, it is becoming acknowledged as a nutritionally significant bioactive chemical that boosts the functional value of foods. The use of BCP primarily arises from spices and aromatic herbs, where it enhances fvor, aroma, and preservation due to its antioxidant and antibacterial characteristic (4, 5). It has attracted considerable interest due to its antioxidant, anti-inflammatory, and cytoprotective properties (6-8).

Paclitaxel (PTX) is a microtubule-stabilizing chemotherapeutic agent widely used in the treatment of solid tumors, including breast, ovarian, and lung cancers. Despite its clinical efficacy, PTX is associated with significant off-target toxicities that compromise patient quality of life. Among these adverse effects, male reproductive toxicity has received increasing attention, as PTX exposure has been linked to

impaired spermatogenesis, hormonal imbalance, and long-term fertility dysfunction (9-11). However, the molecular mechanisms underlying PTX-induced testicular injury remained incompletely understood, limiting the development of effective protective strategies. Accumulating evidence indicates that oxidative stress and mitochondrial dysfunction play central roles in chemotherapy-induced reproductive damage (12-14). Testicular tissue is particularly vulnerable to oxidative insults due to its high rate of cell proliferation, abundance of polyunsaturated fatty acids, and limited antioxidant capacity. Excessive generation of ROS disrupts mitochondrial homeostasis, induces oxidative DNA damage, and activates inflammatory and apoptotic signaling cascades, ultimately leading to germ cell loss and testicular fibrosis (15, 16). Paclitaxel has been shown to exacerbate these processes by impairing endogenous antioxidant defenses and promoting mitochondrial ROS accumulation. The AMPK pathway serves as a critical cellular energy sensor and regulator of mitochondrial integrity. AMPK activates downstream targets involved in redox balance and stress adaptation, including SIRT3, a mitochondrial deacetylase that governs antioxidant enzyme activity. SIRT3 directly regulates MnSOD, a key mitochondrial antioxidant enzyme responsible for detoxifying superoxide radicals (17). In parallel, Nrf2 orchestrates the transcriptional activation of antioxidant and cytoprotective genes (18). Disruption of the p-AMPK/SIRT3/Nrf2 axis implicated in oxidative stress-driven tissue injury; however, its involvement in PTX-induced testicular toxicity is not fully elucidated.

Emerging studies suggest that BCP can modulate redox-sensitive signaling pathways and attenuate oxidative tissue damage in experimental models of inflammation and toxicity. However, the mechanism of BCP to protect against chemotherapy-induced testicular injury, via regulating mitochondrial antioxidant signaling, remains largely unexplored. In this study, we investigated the protective effects of BCP against paclitaxel-induced testicular toxicity using a comprehensive experimental approach. We examined oxidative stress markers, including total SOD, MnSOD, catalase, lipid peroxidation, and oxidative DNA damage, alongside inflammatory cytokines, apoptotic signaling, and histopathological alterations. Furthermore, we assessed reproductive functional endpoints, such as serum testosterone levels, testicular coefficient, and sperm quality parameters. Importantly, we focused on delineating the role of the p-AMPK/SIRT3/Nrf2 signaling axis in mediating the protective actions of PCB. Our findings provide mechanistic insight into chemotherapy-associated male reproductive toxicity and identify PCB as a potential adjunctive strategy for preserving testicular function during anticancer therapy.

2. Methods

2.1. Chemicals

Paclitaxel (PTX) and β-caryophyllene (BCP) came from Sigma-Aldrich (St. Louis, MO, USA). Antibodies for Western blotting and immunohistochemistry were sourced from Thermo Fisher Scientific (Waltham, MA, USA), and the TUNEL kit for apoptosis detection was obtained from Elabscience (Houston, TX, USA). Remaining chemicals and reagents were analytical grade from common commercial sources.

2.2. Animals

Thirty male Swiss albino mice (6–8 weeks, 22–25 g) were supplied by King Saud University's animal house in Riyadh, Saudi Arabia. These pathogen-free, healthy mice acclimatized for one week in standard conditions (25 ± 2 °C, 60–70% humidity, 12 h light/dark cycle) within polypropylene cages, with unlimited access to chow and water. All animal experimental procedures were conducted in strict accordance with the guidelines of the Institutional Animal Care and Use Committee (IACUC) and complied with the ARRIVE 2.0 guidelines. The study was conducted in accordance with internationally accepted ethical standards, including the U.K. Animals (Scientific Procedures) Act, 1986 and its associated guidelines, the EU Directive 2010/63/EU for animal experiments, and the National Institutes of Health Guide for the Care and Use of Laboratory Animals (NIH Publications No. 8023, revised 1978). The experimental protocol was reviewed and approved by the Animal Research Ethics Committee of King Faisal University, in accordance with the Declaration of King Faisal University, and approved by the Institutional Review Board (IRB) under approval number ETHICS3761.

2.3. Experimental Setup

Post-acclimatization, mice were split randomly into five groups (n = 6/group): Group I (control), Group II (PTX), Group III (PTX + BCP 25 mg/kg), Group IV (PTX + BCP 50 mg/kg), Group V (BCP 50 mg/kg alone). PTX dosing totaled 2 mg/kg weekly (1 mg/kg twice weekly) over eight weeks, while BCP was given daily at noted doses for the full period, concurrently in combination groups. Daily monitoring tracked health, intake, body weight, and distress; no endpoints or incidents occurred. Humane euthanasia at endpoint enabled collection of blood and tissues for assays. Cages and dosing order were consistent but not randomized, with uniform housing; assessors for histopathology, biochemistry, blots, and sperm metrics stayed blinded

2.4. Reproductive Parameters

Testes were removed post-euthanasia, cleared of fat, weighed accurately against final body weights, and testicular coefficient derived as testis weight/body weight (%).Sperm counts used cauda epididymis minced in 1 mL warm saline (37 °C), rested 5 min, diluted, and tallied on Neubauer chamber at ×400, reported in $\times 10^6$/mL. Motility checked fresh drops on warm slides at ×400, scoring ≥200 sperm as % motile. Viability applied eosin-nigrosin to aliquots, air-dried smears viewed at ×400 (≥200 sperm), live (unstained) vs. dead (pink/red) as % live. Serum testosterone derived from clotted blood spun at 3,000 rpm (10 min), frozen at −80 °C, and ELISA-quantified at 450 nm (ng/mL).

2.5. Oxidative Damage Assays

8-OHdG ELISA gauged testicular DNA oxidation from PBS-homogenates centrifuged (10,000 × g, 4 °C, 10 min), normalized to protein (ng/mg). MnSOD activity used WST kit with KCN to suppress Cu/Zn-SOD on buffer supernatants (10,000 × g, 4 °C), read at 450 nm (U/mg protein). Total SOD mirrored WST sans KCN on same preps (U/mg protein). MDA quantified lipid damage via thiobarbituric acid on homogenates, heated/cooled/spun, read at 532 nm vs. standards (nmol/mg protein).

2.6. Blotting Technique

Westerns lysed tissues in cold RIPA plus inhibitors, spun (12,000 × g, 4 °C, 15 min), BCA-dosed, SDS-PAGE separated, PVDF-transferred, milk-blocked, overnight primary-probed (p-AMPK/AMPK, SIRT3, Nrf2, apoptosis markers) at 4 °C, HRP-secondary incubated, ECL-detected, β-actin-normalized densitometry.

2.7. Histology

Tissues fixed in 10% formalin, ethanol-dehydrated, xylene-cleared, paraffin-embedded, 5 µm-sectioned, H&E-stained post-dewax/rehydrate, microscoped for structure/tubules/germ cells. IHC deparaffinized sections antigen-retrieved (citrate), H_2O_2-quenched, serum-blocked, primary-overnight (4 °C), secondary-applied, DAB-chromogenic, hematoxylin-counterstained, blinded scoring. TUNEL kit-processed sections deparaffinized/proteinase-K-treated, reaction-labeled DNA nicks, fluoresced/chromogen-visualized, random-field quantified positives. Masson's trichrome deparaffinized/rehydrated sections hematoxylin/fuchsin/aniline blue-stained collagen blue, assessed fibrosis microscopically.

2.8. Statistics

Results show mean ± SD via GraphPad Prism 9.0 one-way ANOVA + Tukey's test: $p < 0.05$ (* vs. control; @ vs. PTX), $p < 0.01$ (# vs. PTX).

3. Results

3.1. BCP ameliorates paclitaxel-induced reproductive dysfunction

Figure 1A shows the chemical structure of BCP, a bicyclic sesquiterpene employed in this work. PTX treatment significantly reduced testicular coefficient compared to the control group ($p < 0.05$), indicating atrophy and compromised gonadal integrity (Figure 1B). BCP co-treatment dramatically restored testicular coefficient in a dose-dependent manner, with the high-dose group outperforming the PTX group ($p < 0.01$). BCP did not change testicular coefficient compared to controls. In Figure 1C, PTX exposure significantly reduced sperm count compared to controls ($p < 0.05$). The high dose of BCP co-administration considerably improved sperm concentration compared to PTX ($p < 0.01$), approaching control values. BCP alone did not reduce sperm. Sperm motility considerably reduced in the PTX group compared to controls ($p < 0.05$; Figure 1D). Both low- and high-dose BCP treatments dramatically improved sperm motility in mice compared to PTX, with the high-dose group showing a significant effect ($p < 0.01$). No significant change found between BCP-alone and control groups. Sperm viability analysis showed a significant decrease in living sperm after PTX therapy ($p < 0.05$ vs. control; Figure 1E). Higher doses of BCP supplementation significantly enhanced sperm vitality, with high-dose BCP exhibiting a stronger protective effect than PTX ($p < 0.01$). BCP alone kept sperm alive. Serum testosterone levels in PTX-treated mice considerably lower than controls ($p < 0.05$; Figure 1F), confirming Leydig cell malfunction. High-dose BCP co-treatment significantly increased testosterone levels compared to PTX ($p < 0.01$). BCP-alone animals had equivalent testosterone levels to controls. These data show that BCP

successfully mitigates paclitaxel-induced reproductive dysfunction by retaining testicular bulk, enhancing sperm quality, and restoring androgen production.

3.2. BCP Suppresses Paclitaxel-Induced Pro-Inflammatory Cytokine Expression in Renal Tissue

Western blot examination demonstrated that PTX administration significantly elevated the protein expression of TNF-α, IL-6, and IL-1β in renal tissue relative to the control group ($p < 0.05$; Figure 2A). These findings demonstrate a significant inflammatory response subsequent to PTX administration. Co-treatment with BCP markedly reduced the PTX-induced elevation of these pro-inflammatory cytokines in a dose-dependent fashion. Quantitative densitometric analysis revealed that low-dose BCP considerably decreased TNF-α, IL-6, and IL-1β protein levels in comparison to the PTX group ($p < 0.05$), whereas high-dose BCP resulted in a markedly significant reduction in cytokine expression ($p < 0.01$; Figure 2B). Significantly, renal tissues from animals administered just with BCP demonstrated cytokine expression levels akin to those of the control group, suggesting that BCP did not provoke a pro-inflammatory response in physiological conditions. These data collectively indicate that BCP efficiently alleviates paclitaxel-induced kidney inflammation by inhibiting essential pro-inflammatory cytokines.

3.3. BCP Mitigates Oxidative Stress and DNA Damage in Testicular Tissue Induced by Paclitaxel

Figure 3A illustrates that PTX administration resulted in a notable elevation of testicular 8-OHdG levels relative to the control group ($p < 0.05$), signifying increased oxidative DNA damage. The co-administration of BCP markedly diminished 8-OHdG levels in a dose-dependent fashion, with the high-dose BCP cohort demonstrating a statistically significant drop compared to the PTX group ($p < 0.01$). The evaluation of lipid peroxidation indicated that MDA levels significantly increased in the PTX group relative to the control group ($p < 0.05$; Figure 3B). BCP treatment markedly reduced PTX-induced lipid peroxidation, with high-dose BCP normalizing MDA levels to near those of the control group ($p < 0.01$ vs. PTX). In accordance with heightened oxidative stress, total SOD activity markedly reduced in PTX-treated animals relative to controls ($p < 0.05$; Figure 3C). BCP supplementation markedly reinstated total SOD activity, with a more substantial impact at the elevated dosage ($p < 0.01$ compared. PTX). Mitochondrial MnSOD activity significantly diminished after PTX administration ($p < 0.05$ vs. control; Figure 3D), suggesting impaired mitochondrial antioxidant defense. BCP co-treatment markedly increased MnSOD activity in a dose-dependent fashion, with the high-dose BCP resulting in a statistically significant restoration relative to the PTX group ($p < 0.01$). The immunohistochemical investigation confirmed the biochemical results. Figure 3E illustrates that PTX-treated testes displayed significant 8-OHdG staining in seminiferous tubules, indicating substantial oxidative DNA damage. Conversely, the BCP-treated groups had significantly decreased 8-OHdG staining intensity, especially in the high-dose cohort, but the testes from the BCP-alone group demonstrated staining patterns akin to the controls. These findings indicate that BCP efficiently alleviates paclitaxel-induced oxidative stress and DNA damage by inhibiting lipid peroxidation and reinstating total and mitochondrial antioxidant enzyme activity.

3.4. BCP Activates Nrf2-Mediated Antioxidant Signaling in Paclitaxel-Induced Testicular Injury

Western blot analysis revealed that PTX treatment markedly reduced the protein expression of Nrf2 and its downstream antioxidant targets HO-1 and NQO-1 in testicular tissue compared to the control group ($p < 0.05$; Figure 4A). This decrease signifies a compromise of the intrinsic antioxidant defense mechanism subsequent to PTX exposure. Co-treatment with BCP significantly reinstated Nrf2 signaling in a dose-dependent way. Quantitative densitometric analysis demonstrated that low-dose BCP considerably elevated the expression of Nrf2, HO-1, and NQO-1 proteins compared to the PTX group ($p < 0.05$), but high-dose BCP resulted in a markedly significant overexpression of these antioxidant proteins ($p < 0.01$; Figure 4B). Significantly, BCP injection alone did not markedly change the basal expression levels of Nrf2, HO-1, or NQO-1 in comparison to control animals, suggesting that BCP does not provoke inappropriate activation of antioxidant signaling under physiological settings. The findings indicate that BCP efficiently mitigates paclitaxel-induced oxidative stress by reactivating the Nrf2-dependent antioxidant defense mechanism, along with the observed restoration of MnSOD activity and reduction of oxidative DNA damage.

3.5. β-Caryophyllene Preserves Testicular Histological Architecture in Paclitaxel-Treated Mice

Histopathological analysis of hematoxylin and eosin (H&E)–stained testicular sections demonstrated well-structured seminiferous tubules in the control group (Group I), marked by systematically arranged seminiferous tubules (ST) with an intact basement membrane and uniformly organized germinal epithelium (Figure 5). Spermatogonia manifested as big, densely pigmented cells near to the basement membrane, whereas initial spermatocytes displayed nuclei positioned centrally. Secondary spermatocytes and spermatids exhibited pale cytoplasm, while mature spermatozoa with distinctly lengthened tails were plainly observable within the tubular lumen. The interstitial space (IS) is thin and contains typical stromal components. Conversely, the paclitaxel-treated group (Group II) demonstrated significant degenerative alterations in the majority of seminiferous tubules, characterized by the loss of normal tubular architecture, detachment of spermatogenic cells from the basement membrane, expansion of the interstitial space, and degradation of the germinal epithelium. Aggregation of many spermatozoa and exfoliated germ cells within the tubular lumen is apparent. Numerous seminiferous tubules exhibited necrosis and demonstrated significant cytoplasmic vacuolation. Furthermore, engorged and expanded blood vessels, together with significant infiltration of mononuclear inflammatory cells, were noted, signifying severe testicular damage. Co-treatment with low-dose β-caryophyllene (Group III) led to partial maintenance of seminiferous tubule architecture. While several tubules displayed structured germinal epithelium, degenerative tubules with a shrunken appearance, cytoplasmic vacuolation, modest expansion of interstitial gaps, and isolated atrophy of the germinal epithelium were still apparent. Disorganization of germ cell layers within the afflicted tubules, together with clogged blood arteries and modest infiltration of inflammatory cells, was also seen. In the high-dose β-caryophyllene group (Group IV), testicular architecture significantly enhanced relative to the PTX group. The majority of seminiferous tubules exhibited nearly normal arrangement of spermatogenic cell layers with few degenerative alterations. The interstitial gaps were narrow, inflammatory cell infiltration was diminished, and vascular congestion was limited. Intermittent desquamation of immature germ cells into the tubular lumen was noted; nonetheless, the general integrity of the testis remains essentially intact.

Testes from animals administered β-caryophyllene only (Group V) exhibited intact seminiferous tubule architecture and normal spermatogenic organization in the majority of tubules. The germinal epithelium remained intact, with only slight enlargement of interstitial gaps observed, suggesting that β-caryophyllene did not cause detrimental histological changes.

3.6. BCP Restores p-AMPK and SIRT3 Signaling in Paclitaxel-Induced Testicular Injury

To investigate whether BCP modulates upstream mitochondrial stress–response signaling, we assessed the protein expression of p-AMPK and SIRT3 in testicular tissue by Western blotting. As shown in Figure 6A, paclitaxel (PTX) treatment significantly reduced p-AMPK levels compared with the control group ($p < 0.05$), indicating suppression of AMPK activation. PTX exposure also markedly downregulated SIRT3 expression in the testes ($p < 0.05$ vs. control), consistent with impaired mitochondrial antioxidant regulation. BCP co-treatment significantly and dose-dependently restored the expression of both p-AMPK and SIRT3 compared with the PTX group. Densitometric quantification demonstrated that low-dose BCP significantly increased p-AMPK and SIRT3 levels relative to PTX ($p < 0.05$), whereas high-dose BCP produced a highly significant restoration of these proteins ($p < 0.01$; Figure 6B), approaching control values. BCP alone did not significantly alter basal p-AMPK or SIRT3 levels relative to controls. Taken together, these results suggest that BCP mitigates PTX-induced testicular injury, at least in part, by reactivating the p-AMPK/SIRT3 signaling axis, which is consistent with the observed restoration of MnSOD activity and reactivation of Nrf2-dependent antioxidant proteins.

3.8. BCP Attenuates Paclitaxel-Induced Testicular Apoptosis

Apoptotic signaling in testicular tissue was evaluated by assessing the expression of the anti-apoptotic protein Bcl-2 and the executioner enzyme cleaved caspase-3 using Western blotting. Figure 7A illustrates that PTX treatment drastically reduced Bcl-2 expression and markedly elevated cleaved caspase-3 levels relative to the control group ($p < 0.05$), indicating the activation of apoptotic pathways in the testes. Densitometric analysis corroborated these results (Figure 7B), revealing a considerable downregulation of Bcl-2 and a simultaneous elevation of cleaved caspase-3 in the PTX group. Co-treatment with BCP markedly and dose-dependently rectified these changes. Low-dose BCP markedly reinstated Bcl-2 expression and diminished cleaved caspase-3 levels in comparison to PTX ($p < 0.05$), but high-dose BCP resulted in a highly substantial normalization of both apoptotic indicators ($p < 0.01$). BCP alone did not markedly influence apoptotic protein expression compared to control mice. Apoptotic cell death was further assessed utilizing the TUNEL test. Figure 7C demonstrates that PTX-treated testes displayed a significant rise in TUNEL-positive nuclei within seminiferous tubules, signifying widespread DNA breakage and apoptosis. Conversely, BCP co-treatment significantly decreased the quantity of TUNEL-positive cells in a dose-dependent fashion, with the high-dose BCP group exhibiting minimal apoptotic labeling akin to controls. These data collectively indicate that BCP efficiently mitigates PTX-induced testicular apoptosis, presumably by reinstating mitochondrial antioxidant signaling and obstructing caspase-dependent cell death pathways.

3.9. BCP Attenuates Paclitaxel-Induced Testicular Fibrosis

Masson's trichrome staining was conducted to assess collagen deposition and fibrotic remodeling in testicular tissue. Figure 8 illustrates that control testes displayed normal histoarchitecture, with limited collagen deposition localized to the peritubular and interstitial areas. Conversely, PTX-treated testes exhibited significant fibrotic alterations, evidenced by strong blue-stained collagen deposition, thickening of interstitial spaces, and disorganization of seminiferous tubules, signifying substantial testicular fibrosis. Co-treatment with BCP substantially reduced PTX-induced fibrotic changes in a dose-dependent fashion. The low-dose BCP group exhibited a significant decrease in collagen deposition and partial maintenance of seminiferous tubule architecture, whereas the high-dose BCP group revealed a pronounced reduction in fibrotic remodeling, with collagen distribution nearing that of control testes. Testes from animals administered just with BCP displayed normal histological characteristics with no collagen deposition, akin to the control group. The data demonstrate that BCP successfully mitigates paclitaxel-induced testicular fibrosis, aligning with its capacity to diminish oxidative stress, inflammation, and apoptosis, thus maintaining testicular structural integrity.

4. Discussion

Paclitaxel (PTX), a potent chemotherapy drug, has a major limitation of testicular damage in clinical settings (19). Research increasingly points to oxidative stress-induced mitochondrial impairment, inflammation, cell death, and tissue scarring as key drivers of testicular harm from chemotherapy (20). This study reveals how BCP offers strong safeguards against PTX-related testicular damage by fine-tuning mitochondrial redox balance, boosting antioxidant systems, curbing inflammation, and blocking cell death pathways. Testicular cells are especially prone to oxidative harm because of their intense energy demands and the high levels of fragile fatty acids in sperm membranes (21). As seen in prior studies, PTX sharply raises markers of fat breakdown (malondialdehyde, or MDA) and DNA oxidation (8-OHdG), while draining natural antioxidants (22, 23). This oxidative assault triggers germ cell loss and disrupts sperm production, mirroring patterns in PTX toxicity models. BCP, however, effectively curbs these markers, showing its power to counteract PTX-driven oxidative injury.

A key discovery is BCP's ability to revive mitochondrial antioxidant defenses, especially by restoring MnSOD function. This enzyme, located in mitochondria, neutralizes superoxide from energy production (24). Weak MnSOD leads to excess mitochondrial ROS, harming sperm DNA and fertility. In BCP-treated animals, boosted MnSOD aligned with better tissue structure, less DNA damage, and improved sperm health, highlighting mitochondrial redox control's role in fertility protection. This effect traces back to the p-AMPK/SIRT3 pathway, which governs mitochondrial balance. AMPK activation boosts SIRT3, which activates MnSOD by deacetylation to cut ROS. PTX suppresses p-AMPK and SIRT3 in testes, undermining mitochondrial upkeep (25). BCP dose-dependently revives these proteins, positioning the AMPK–SIRT3–MnSOD pathway as a core way it maintains mitochondrial health amid chemo stress.

BCP also ramps up Nrf2 signaling, the main controller of antioxidant responses. PTX lowers Nrf2 and targets like HO-1 and NQO-1, worsening damage. BCP restores this Nrf2/HO-1/NQO-1 system, strengthening defenses against oxidative and inflammatory harm. This combined action on

mitochondrial (AMPK/SIRT3/MnSOD) and nuclear (Nrf2) pathways shows BCP's comprehensive antioxidant strategy (26). Testicular inflammation often follows oxidative and mitochondrial issues. PTX elevates cytokines like TNF-α, IL-6, and IL-1β, which hinder sperm development and hormone production in Leydig cells, alongside immune cell influx and blood vessel issues. BCP cuts these cytokines and infiltration, leveraging its anti-inflammatory effects likely by first taming oxidative stress (26). Prolonged stress from oxidation and inflammation drives germ cell suicide (27). PTX boosts cleaved caspase-3, drops protective Bcl-2, and raises TUNEL-detected dead cells, firing up mitochondrial death signals. BCP reverses these, implying that steadying redox balance and inflammation jointly prevents cell loss.

Tissue exams and Masson's trichrome staining back this up. PTX causes tubule breakdown, tissue swelling, immune invasion, and heavy collagen buildup signaling fibrosis. BCP protects tubule integrity, limits scarring, and yields functional gains like normalized testis weight, testosterone, and sperm metrics. Overall, PTX harms testes by blocking p-AMPK/SIRT3/MnSOD and Nrf2 defenses, sparking oxidation, inflammation, death, and fibrosis. BCP reverses this via pathway reactivation, cytokine dampening, and apoptosis blockade, safeguarding structure and fertility. As a safe, diet-sourced compound commonly consumed by people, BCP holds promise as a nutraceutical or food additive to ease chemo's fertility toll. Though animal data needs human validation, these findings justify deeper studies in nutrition, translation, and clinics.

5. Conclusion

This work illustrates that paclitaxel causes significant testicular toxicity marked by oxidative stress, mitochondrial dysfunction, inflammation, apoptosis, and fibrotic remodeling, ultimately resulting in compromised spermatogenesis and hormonal dysregulation. β-Caryophyllene efficiently mitigates these harmful consequences by activating the p-AMPK/SIRT3/Nrf2 signaling pathway, reinstating mitochondrial antioxidant defense, inhibiting inflammatory and apoptotic processes, and maintaining testicular architecture and reproductive function. These findings offer mechanistic insight into chemotherapy-induced male reproductive toxicity and propose β-caryophyllene as a viable therapeutic adjuvant for alleviating paclitaxel-induced testicular damage.

Declarations

Author Contributions: For research articles with several authors, a short paragraph specifying their individual contributions must be provided. The following statements should be used “Conceptualization, P.R, and R.S.; methodology, P.R., R.B.A and S.A.R software, E.M.A.; validation, P.R., B.A and G.K.B.; formal analysis, G.K.B, N.K.A; investigation, P.R., G.K.B and D.P ; resources, P.R and R.B.A.; data curation, P.R.; writing—original draft preparation, P.R.; writing—review and editing, B.A and R,S.; visualization, R.S, S.A.R,N.K.A; supervision, P.R.; project administration, P.R.; funding acquisition, P.R. All authors have read and agreed to the published version of the manuscript.

Funding: The authors extend their appreciation to the Deanship of Scientific Research, Vice Presidency for Graduate Studies and Scientific Research, King Faisal University, Saudi Arabia, for funding this research work (Grant number: KFU253945).

Institutional Review Board Statement: This study was conducted according to the guidelines of King Faisal University and the “Executive Regulations for Research Ethics on Living Creatures (Second Edition)”, published by the National Bioethics Committee, Saudi Arabia. All animal care and experimental procedures were approved by the Animal Research Ethics Committee at King Faisal University Declaration of King Faisal University and approved by the Institutional Review Board, ETHICS3761.

Informed Consent Statement: Not applicable.

Data Availability Statement: The data used to support the findings of this study are available from the corresponding author upon request.

Conflicts of Interest: The authors declare no conflicts of interest.

References

1. Fidyt K, Fiedorowicz A, Strządała L, Szumny A. β-caryophyllene and β-caryophyllene oxide-natural compounds of anticancer and analgesic properties. Cancer medicine. 2016;5(10):3007-17.
2. Eddin LB, Jha NK, Goyal SN, Agrawal YO, Subramanya SB, Bastaki SMA, et al. Health Benefits, Pharmacological Effects, Molecular Mechanisms, and Therapeutic Potential of α-Bisabolol. Nutrients. 2022;14(7).
3. Hashiesh HM, Sharma C, Goyal SN, Sadek B, Jha NK, Kaabi JA, et al. A focused review on CB2 receptor-selective pharmacological properties and therapeutic potential of β-caryophyllene, a dietary cannabinoid. Biomedicine & pharmacotherapy = Biomedecine & pharmacotherapie. 2021;140:111639.
4. Hashiesh HM, Meeran MFN, Sharma C, Sadek B, Kaabi JA, Ojha SK. Therapeutic Potential of β-Caryophyllene: A Dietary Cannabinoid in Diabetes and Associated Complications. Nutrients. 2020;12(10).
5. Gertsch J, Leonti M, Raduner S, Racz I, Chen JZ, Xie XQ, et al. Beta-caryophyllene is a dietary cannabinoid. Proceedings of the National Academy of Sciences of the United States of America. 2008;105(26):9099-104.
6. Hashiesh HM, Azimullah S, Nagoor Meeran MF, Saraswathiamma D, Arunachalam S, Jha NK, et al. Cannabinoid 2 Receptor Activation Protects against Diabetic Cardiomyopathy through Inhibition of AGE/RAGE-Induced Oxidative Stress, Fibrosis, and Inflammasome Activation. The Journal of pharmacology and experimental therapeutics. 2024;391(2):241-57.
7. Olopade EO, Adefegha SA, Alao JO, Adepoju AE, Fakayode AE, Oboh G. Ameliorative Role of β-Caryophyllene on Antioxidant Biomarkers in a Paroxetine-Induced Model of Male Sexual Dysfunction. Basic & clinical pharmacology & toxicology. 2025;136(3):e70010.

8. Mohamed ME, Abdelnaby RM, Younis NS. β-caryophyllene ameliorates hepatic ischemia reperfusion-induced injury: the involvement of Keap1/Nrf2/HO 1/NQO 1 and TLR4/NF-κB/NLRP3 signaling pathways. European review for medical and pharmacological sciences. 2022;26(22):8551-66.
9. Toraman E, Budak B, Bayram C, Sezen S, Mokhtare B, Hacımüftüoğlu A. Role of parthenolide in paclitaxel-induced oxidative stress injury and impaired reproductive function in rat testicular tissue. Chemico-biological interactions. 2024;387:110793.
10. Alhowail AH. Paclitaxel-induced cognitive impairment: mechanistic insights. Frontiers in pharmacology. 2025;16:1684006.
11. Naeem AG, Fawzi SF, Elmorsi RM, George MY. Paclitaxel-induced adverse effects: insights into multi-organ toxicities and molecular mechanisms. Naunyn-Schmiedeberg's archives of pharmacology. 2025.
12. Huot JR, Baumfalk D, Resendiz A, Bonetto A, Smuder AJ, Penna F. Targeting Mitochondria and Oxidative Stress in Cancer- and Chemotherapy-Induced Muscle Wasting. Antioxidants & redox signaling. 2023;38(4-6):352-70.
13. He Y, Zheng J, Ye B, Dai Y, Nie K. Chemotherapy-induced gastrointestinal toxicity: Pathogenesis and current management. Biochemical pharmacology. 2023;216:115787.
14. Zhao P, Guo C, Du H, Xiao Y, Su J, Wang X, et al. Chemotherapy-induced ovarian damage and protective strategies. Human fertility (Cambridge, England). 2023;26(4):887-900.
15. Demir EE, Gur C, Sisman T, Lafzi A, Aksakal Ö. Synthetic cannabinoid CUMYL-4CN-BINACA induces oxidative stress, ER stress, and apoptosis in brain and testicular tissues of male albino rats. Food and Chemical Toxicology. 2025;204:115617.
16. Kankılıç NA, Küçükler S, Gür C, Akarsu SA, Akaras N, Şimşek H, et al. Naringin protects against paclitaxel-induced toxicity in rat testicular tissues by regulating genes in pro-inflammatory cytokines, oxidative stress, apoptosis, and JNK/MAPK signaling pathways. Journal of biochemical and molecular toxicology. 2024;38(7):e23751.
17. Allen AR, Jones A, LoBianco FV, Krager KJ, Aykin-Burns N. Effect of Sirt3 on hippocampal MnSOD activity, mitochondrial function, physiology, and cognition in an aged murine model. Behavioural brain research. 2023;444:114335.
18. Rajendran P, Alzahrani AM, Priya Veeraraghavan V, Ahmed EA. Anti-Apoptotic Effect of Flavokawain A on Ochratoxin-A-Induced Endothelial Cell Injury by Attenuation of Oxidative Stress via PI3K/AKT-Mediated Nrf2 Signaling Cascade. Toxins. 2021;13(11).
19. Genc S, Cicek B, Yeni Y, Kuzucu M, Hacimuftuoglu A, Bolat I, et al. Morinda citrifolia protective effects on paclitaxel-induced testis parenchyma toxicity: An experimental study. Reproductive toxicology (Elmsford, NY). 2024;127:108611.
20. Dutta S, Sengupta P, Slama P, Roychoudhury S. Oxidative Stress, Testicular Inflammatory Pathways, and Male Reproduction. International journal of molecular sciences. 2021;22(18).

21. Asadi N, Bahmani M, Kheradmand A, Rafieian-Kopaei M. The Impact of Oxidative Stress on Testicular Function and the Role of Antioxidants in Improving it: A Review. Journal of clinical and diagnostic research : JCDR. 2017;11(5):Ie01-ie5.
22. Ayala A, Muñoz MF, Argüelles S. Lipid peroxidation: production, metabolism, and signaling mechanisms of malondialdehyde and 4-hydroxy-2-nonenal. Oxidative medicine and cellular longevity. 2014;2014:360438.
23. Mohiuddin M, Kasahara K. The Mechanisms of the Growth Inhibitory Effects of Paclitaxel on Gefitinib-resistant Non-small Cell Lung Cancer Cells. Cancer genomics & proteomics. 2021;18(5):661-73.
24. Iorio R, Celenza G, Petricca S. Multi-Target Effects of ß-Caryophyllene and Carnosic Acid at the Crossroads of Mitochondrial Dysfunction and Neurodegeneration: From Oxidative Stress to Microglia-Mediated Neuroinflammation. Antioxidants (Basel, Switzerland). 2022;11(6).
25. Vahedi Raad M, Firouzabadi AM, Tofighi Niaki M, Henkel R, Fesahat F. The impact of mitochondrial impairments on sperm function and male fertility: a systematic review. Reproductive biology and endocrinology : RB&E. 2024;22(1):83.
26. Loboda A, Damulewicz M, Pyza E, Jozkowicz A, Dulak J. Role of Nrf2/HO-1 system in development, oxidative stress response and diseases: an evolutionarily conserved mechanism. Cellular and molecular life sciences : CMLS. 2016;73(17):3221-47.
27. Ullah H, Di Minno A, Santarcangelo C, Khan H, Daglia M. Improvement of Oxidative Stress and Mitochondrial Dysfunction by β-Caryophyllene: A Focus on the Nervous System. Antioxidants (Basel, Switzerland). 2021;10(4).

Figures

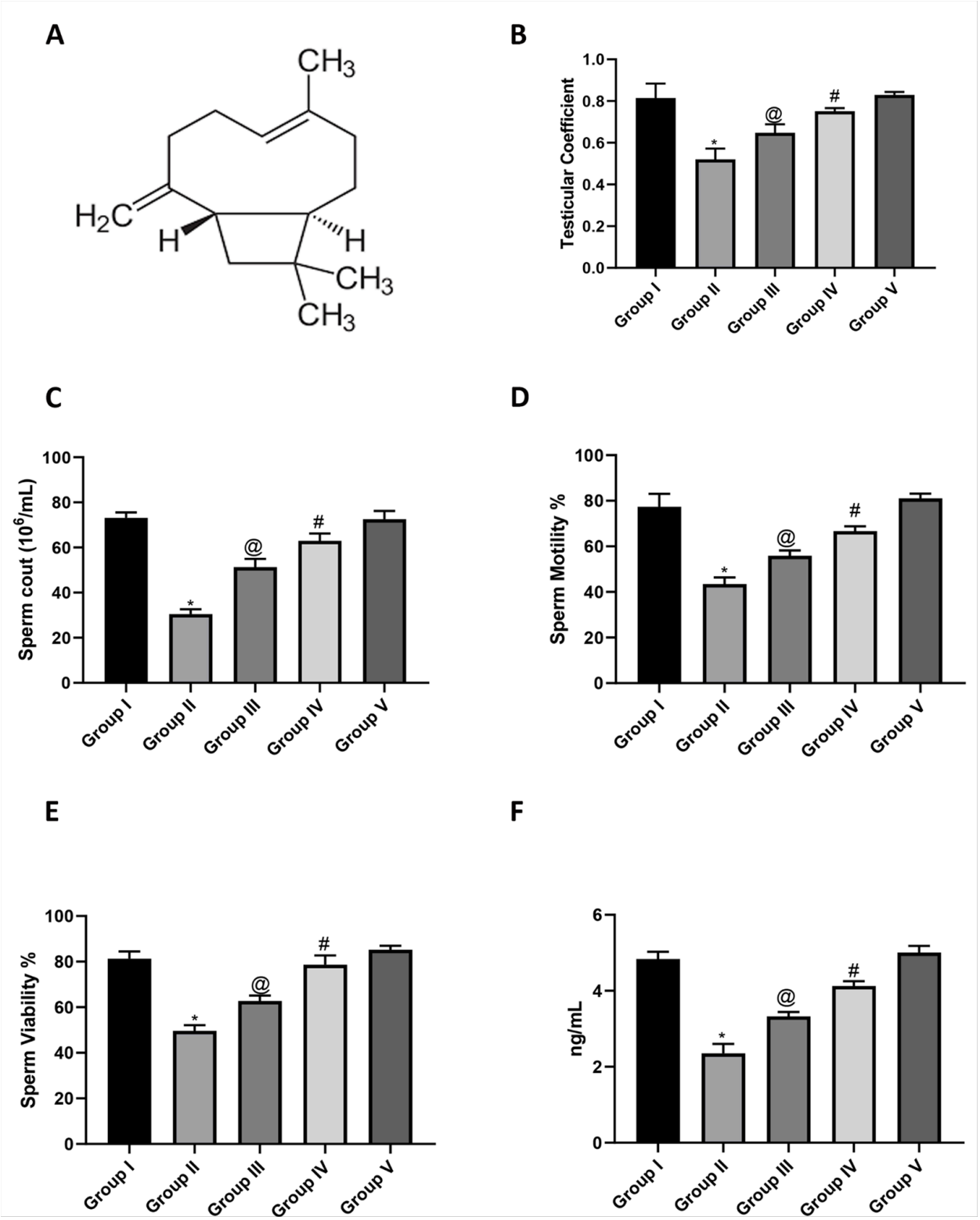

Figure 1

BCP ameliorates paclitaxel-induced reproductive dysfunction. Group I: control, Group II: PTX, Group III: PTX+BCP (25mg/kg) Group IV: PTX+BCP (50mg/kg).Group V: BCP alnoe. (a) Chemical structure of BCP. (b) Testicular coefficient. (c) Sperm count. (d) Sperm motility. (e) Sperm viability. (f) Serum testosterone levels. Data are presented as mean ± SD (n = 6 per group). Statistical analysis performed using one-way

ANOVA followed by Tukey's post hoc test. * p < 0.05 vs. control group; @ p < 0.05 vs. PTX group; # p < 0.01 vs. PTX group.

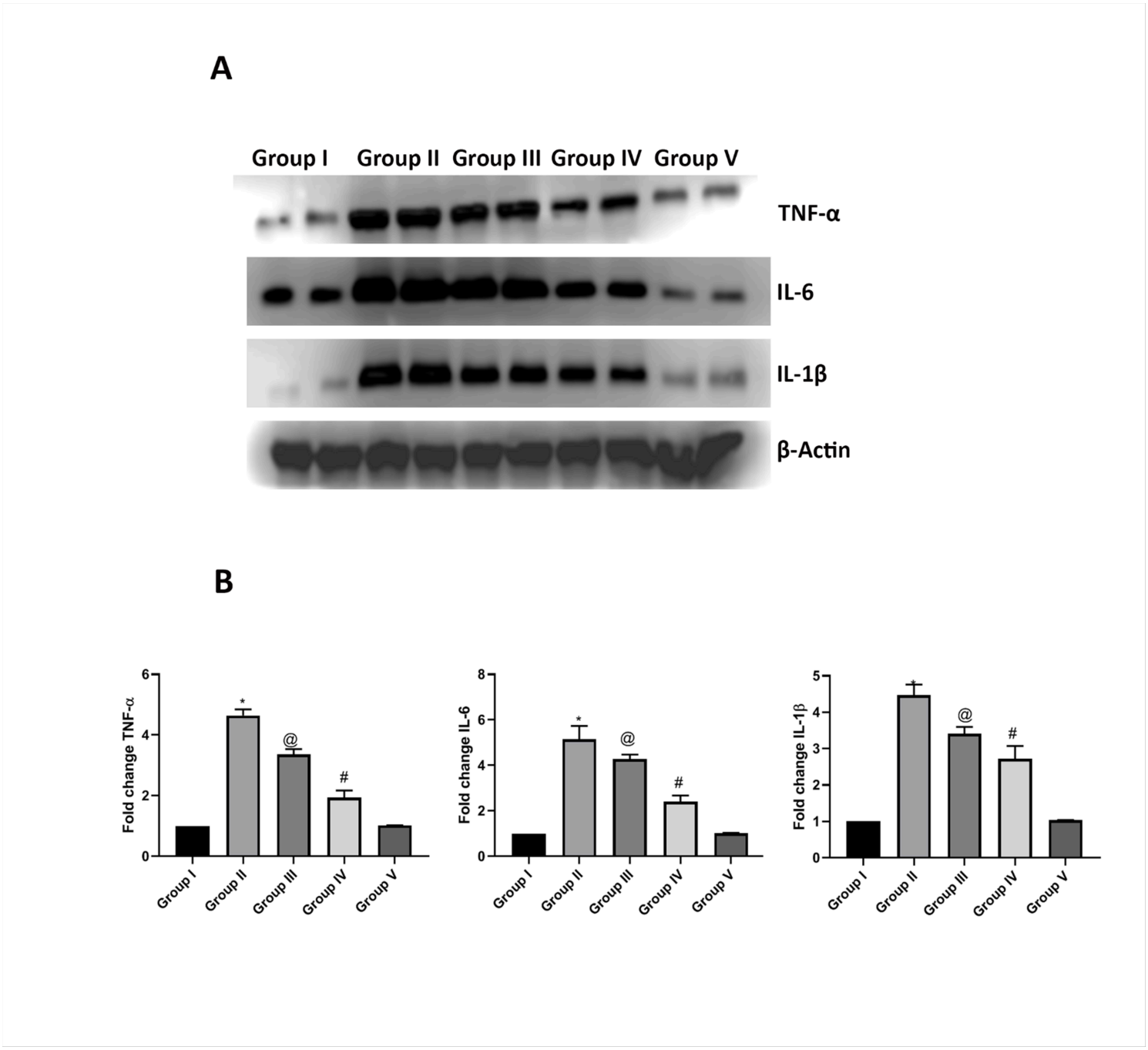

Figure 2

BCP attenuates paclitaxel-induced renal inflammatory cytokine expression. Group I: control, Group II: PTX, Group III: PTX+BCP (25mg/kg) Group IV: PTX+BCP (50mg/kg).Group V: BCP alone. (a) Representative Western blot images showing protein expression of TNF-α, IL-6, and IL-1β in renal tissue across experimental groups. (b) Densitometric analysis of TNF-α, IL-6, and IL-1β protein expression normalized to β-actin. Data are expressed as mean ± SD (n = 6 per group). Statistical analysis performed using one-way ANOVA followed by Tukey's post hoc test. * p < 0.05 vs. control group; @ p < 0.05 vs. PTX group; # p < 0.01 vs. PTX group.

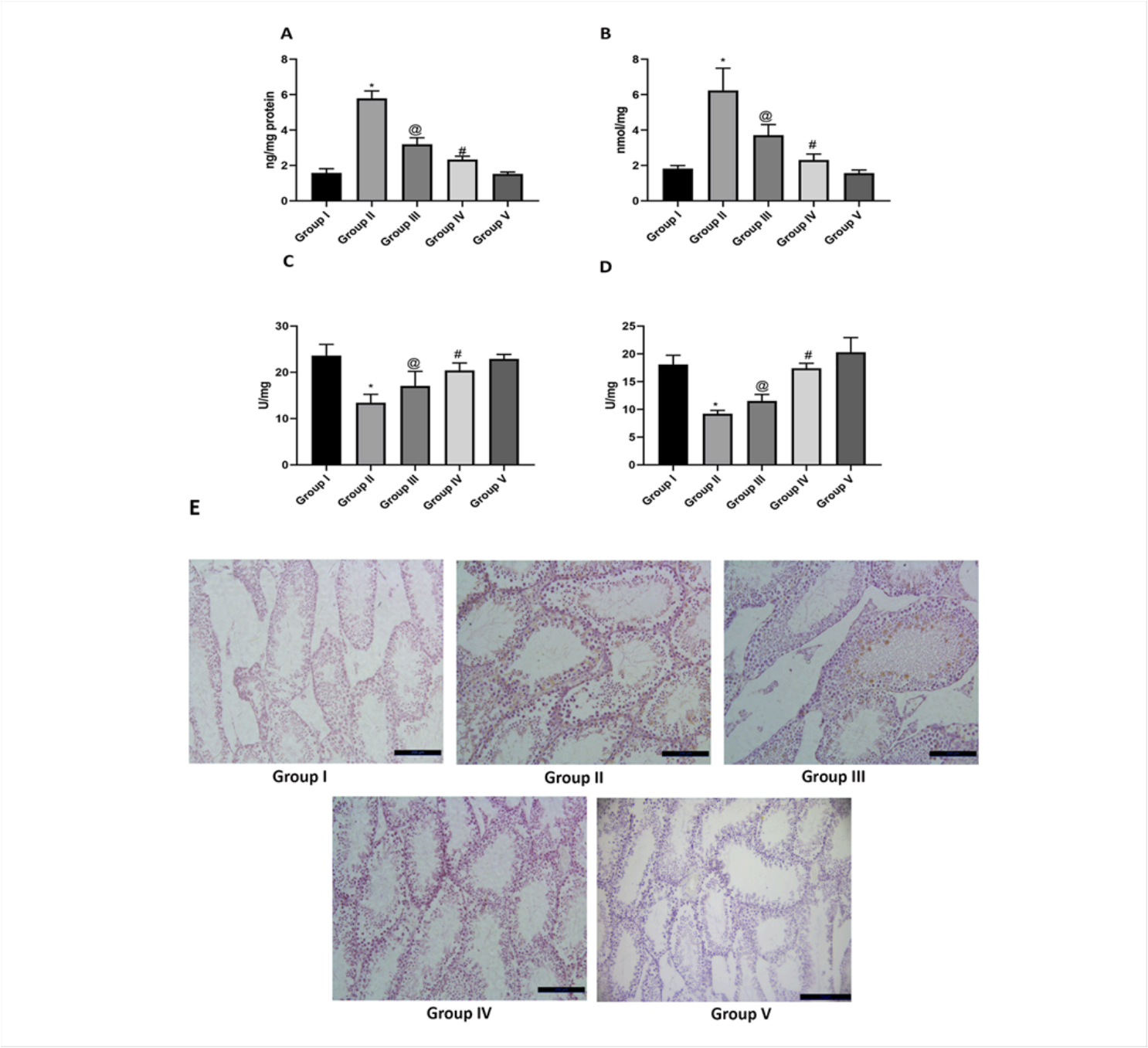

Figure 3

BCP reduces paclitaxel-induced oxidative stress and DNA damage in testicular tissue. Group I: control, Group II: PTX, Group III: PTX+BCP (25mg/kg) Group IV: PTX+BCP (50mg/kg).Group V: BCP alone. (a) Testicular 8-OHdG levels. (b) MDA levels. (c) Total SOD activity. (d) MnSOD activity. (e) Representative immunohistochemical staining showing 8-OHdG expression in testicular tissue (brown staining), with hematoxylin counterstaining of nuclei. Data are expressed as mean ± SD (n = 6 per group). Statistical analysis performed using one-way ANOVA followed by Tukey's post hoc test. * $p < 0.05$ vs. control group; @ $p < 0.05$ vs. PTX group; # $p < 0.01$ vs. PTX group.

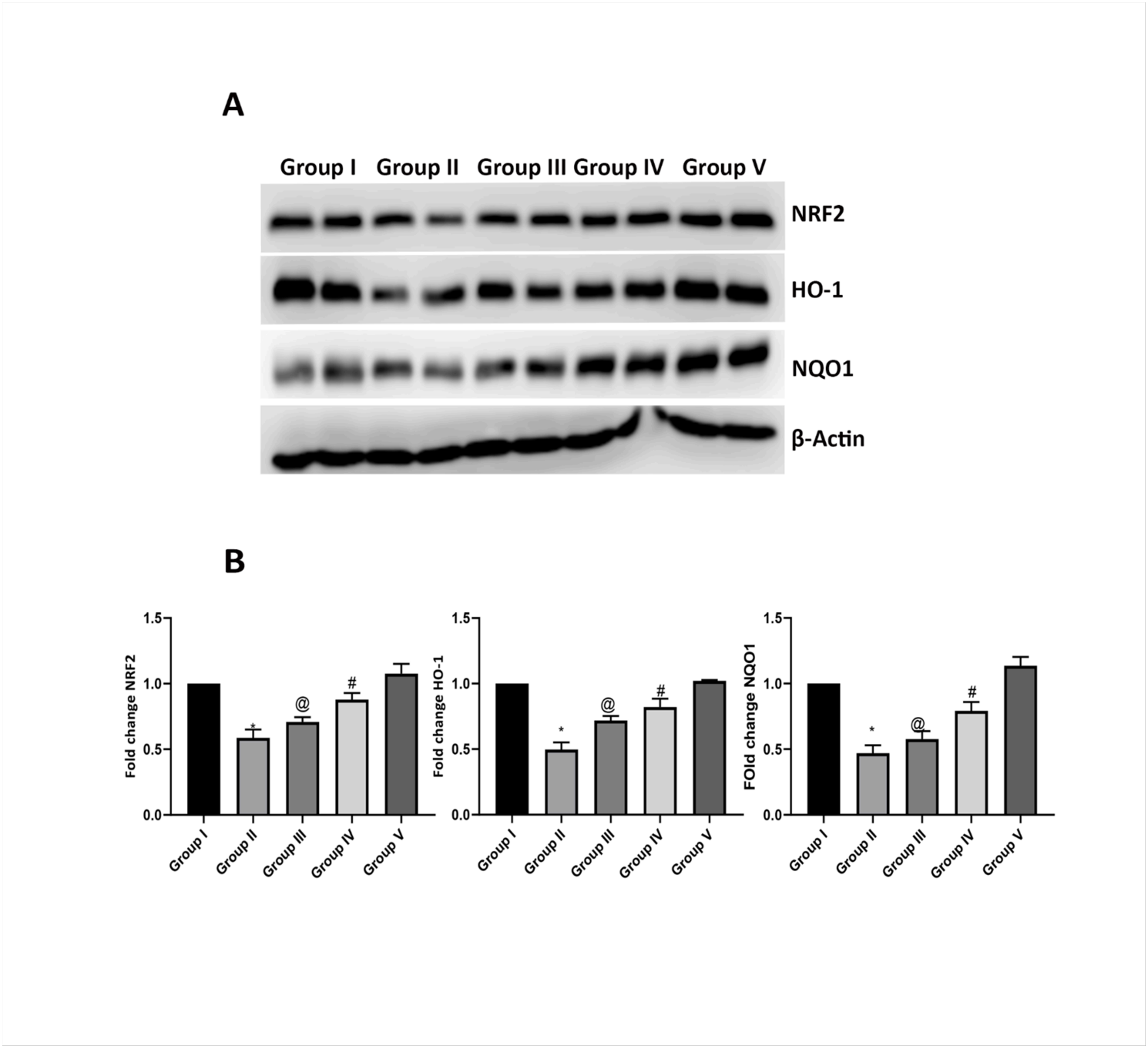

Figure 4

BCP restores Nrf2-dependent antioxidant signaling in paclitaxel-treated testes. Group I: control, Group II: PTX, Group III: PTX+BCP (25mg/kg) Group IV: PTX+BCP (50mg/kg).Group V: BCP alone. (a) Representative Western blot images showing the protein expression of Nrf2, HO-1, and NQO-1 in testicular tissue across experimental groups. (b) Densitometric analysis of Nrf2, HO-1, and NQO-1 protein expression normalized to β-actin. Data are expressed as mean ± SD (n = 6 per group). Statistical analysis performed using one-way ANOVA followed by Tukey's post hoc test. * $p < 0.05$ vs. control group; @ $p < 0.05$ vs. PTX group; # $p < 0.01$ vs. PTX group.

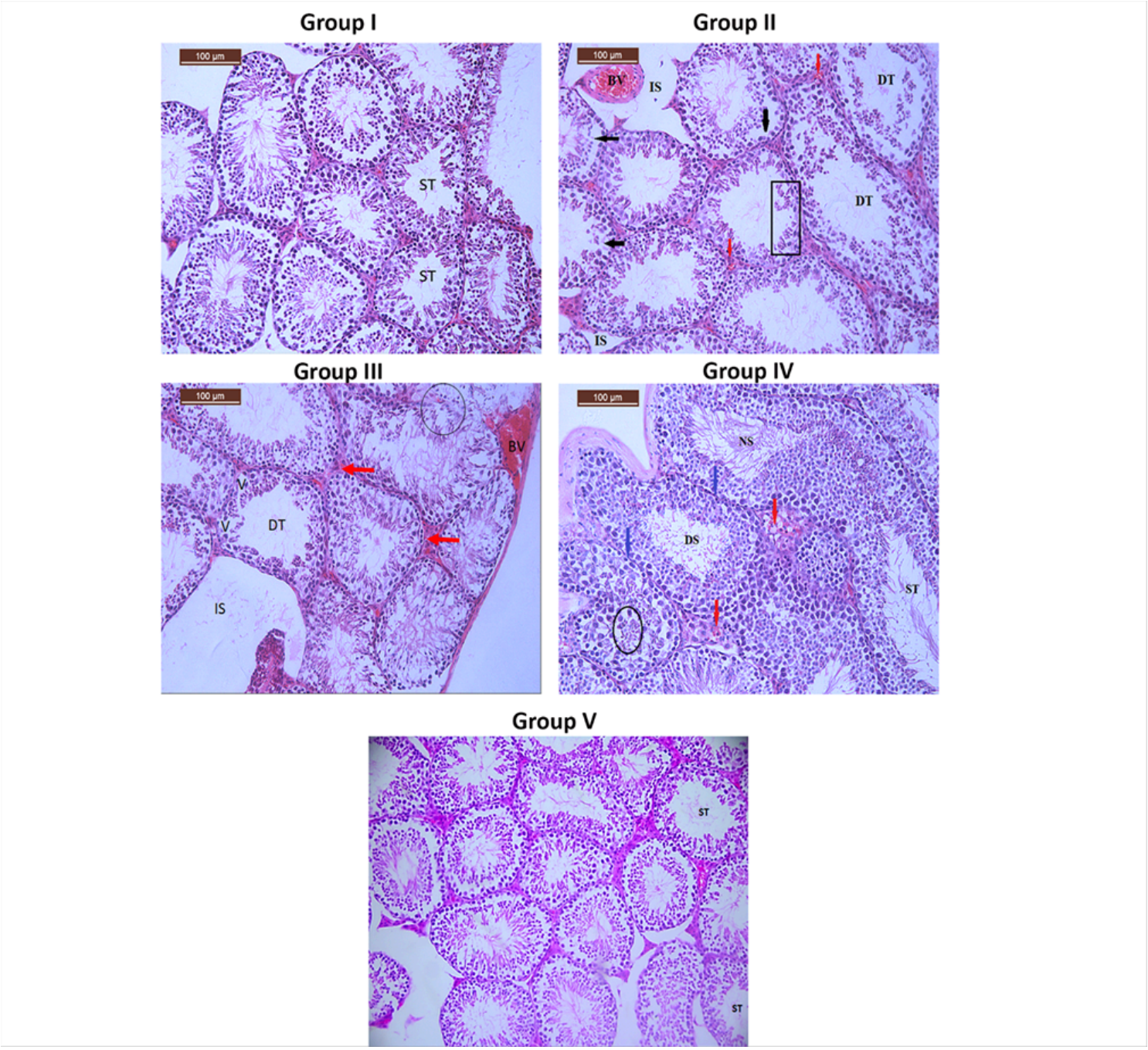

Figure 5

β-Caryophyllene ameliorates paclitaxel-induced histopathological alterations in testicular tissue (H&E staining). Representative photomicrographs of H&E stained testicular sections (×100 magnification). Group I (Control): Regularly arranged seminiferous tubules (ST) with intact germinal epithelium and narrow interstitial space (IS). Group II (PTX): Severe degenerative changes in seminiferous tubules (DT), including loss of tubular architecture, exfoliation of germ cells into the lumen, cytoplasmic vacuolation, widened interstitial spaces (IS), congested blood vessels (BV), and inflammatory cell infiltration (red arrows). Group III (PTX + BCP, 25 mg/kg): Partial restoration of seminiferous tubule architecture with residual degenerative tubules (DT), cytoplasmic vacuolation (V), moderate interstitial widening (IS), focal disorganization of germ cell layers (circle), and mild inflammatory infiltration. Group IV (PTX + BCP, 50

mg/kg): Marked improvement of testicular architecture with well-organized spermatogenic layers, narrow interstitial spaces (blue arrows), minimal inflammatory infiltration, and occasional desquamation of immature germ cells into the tubular lumen (circle). Group V (BCP alone): Preserved seminiferous tubule structure with normal spermatogenic organization and mild interstitial widening (IS).

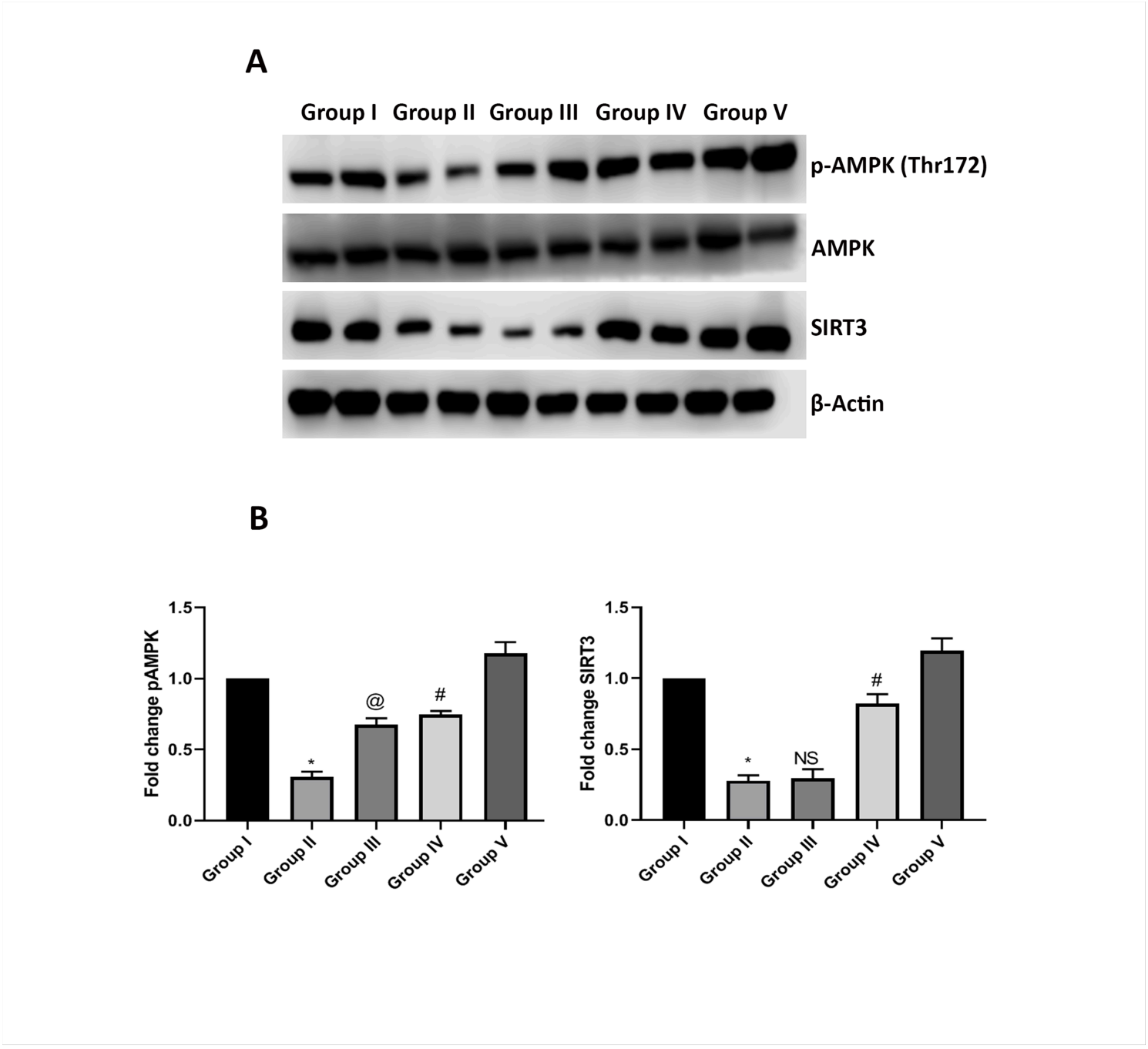

Figure 6

BCP restores p-AMPK/SIRT3 signaling in paclitaxel-treated testes. Group I: control, Group II: PTX, Group III: PTX+BCP (25mg/kg) Group IV: PTX+BCP (50mg/kg). Group V: BCP alone. (a) Representative Western blot images showing p-AMPK and SIRT3 protein expression in testicular tissue across experimental groups. (b) Densitometric quantification of p-AMPK and SIRT3 normalized to β-actin and p-AMPK additionally normalized to total AMPK. Data are expressed as mean ± SD (n = 6 per group).

Statistical analysis performed using one-way ANOVA followed by Tukey's post hoc test. * $p < 0.05$ vs. control group; @ $p < 0.05$ vs. PTX group; # $p < 0.01$ vs. PTX group.

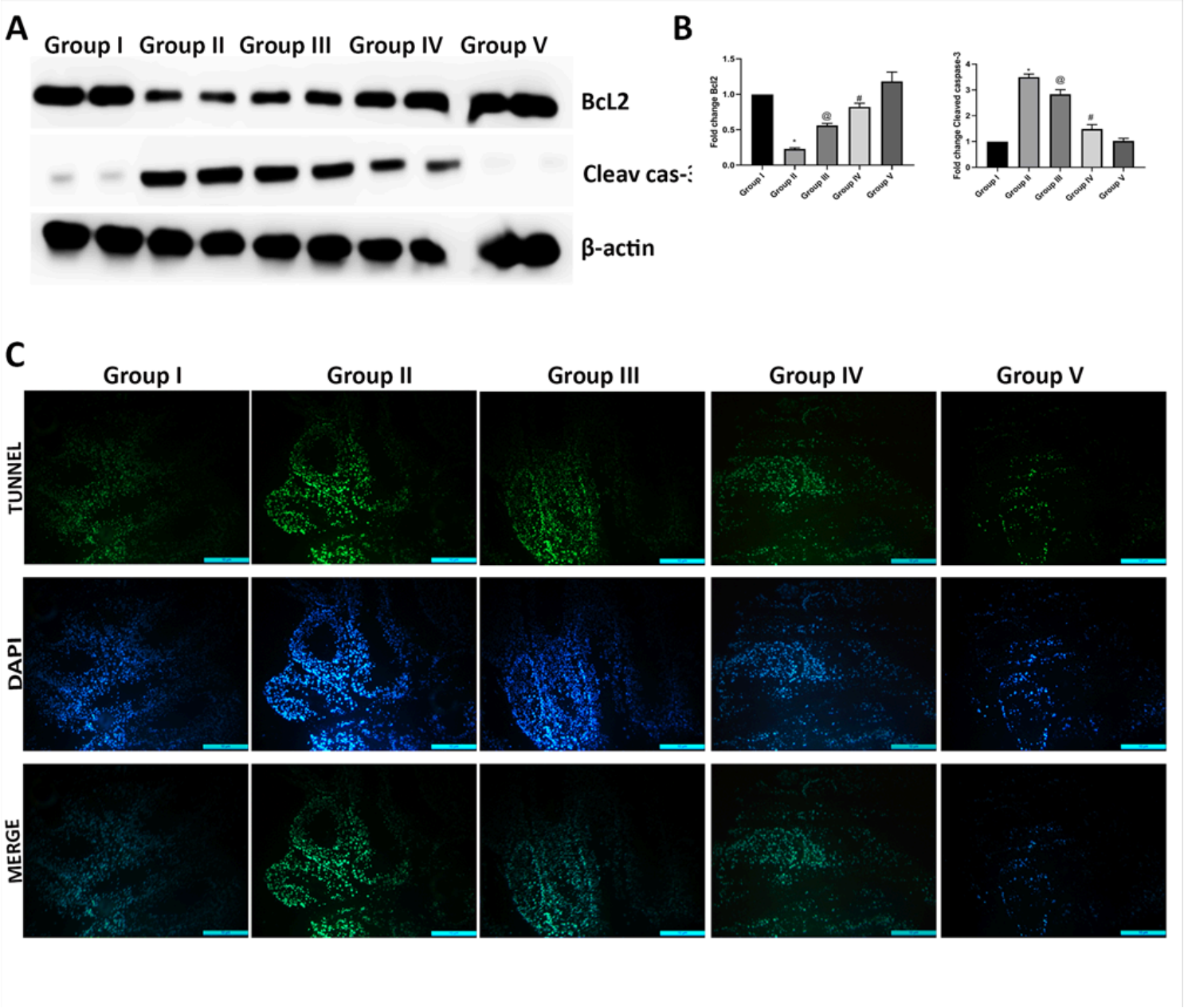

Figure 7

BCP suppresses paclitaxel-induced apoptosis in testicular tissue. Group I: control, Group II: PTX, Group III: PTX+BCP (25mg/kg) Group IV: PTX+BCP (50mg/kg).Group V: BCP alone. (a) Representative Western blot images showing the expression of Bcl-2 and cleaved caspase-3 in testicular tissue across experimental groups. (b) Densitometry quantification of Bcl-2 and cleaved caspase-3 protein expression normalized to β-actin. (c) Representative TUNEL staining images showing apoptotic nuclei in testicular tissue positive cells indicated by fluorescent staining. Representative photomicrographs of TUNNEL stained testicular sections (×20magnification).

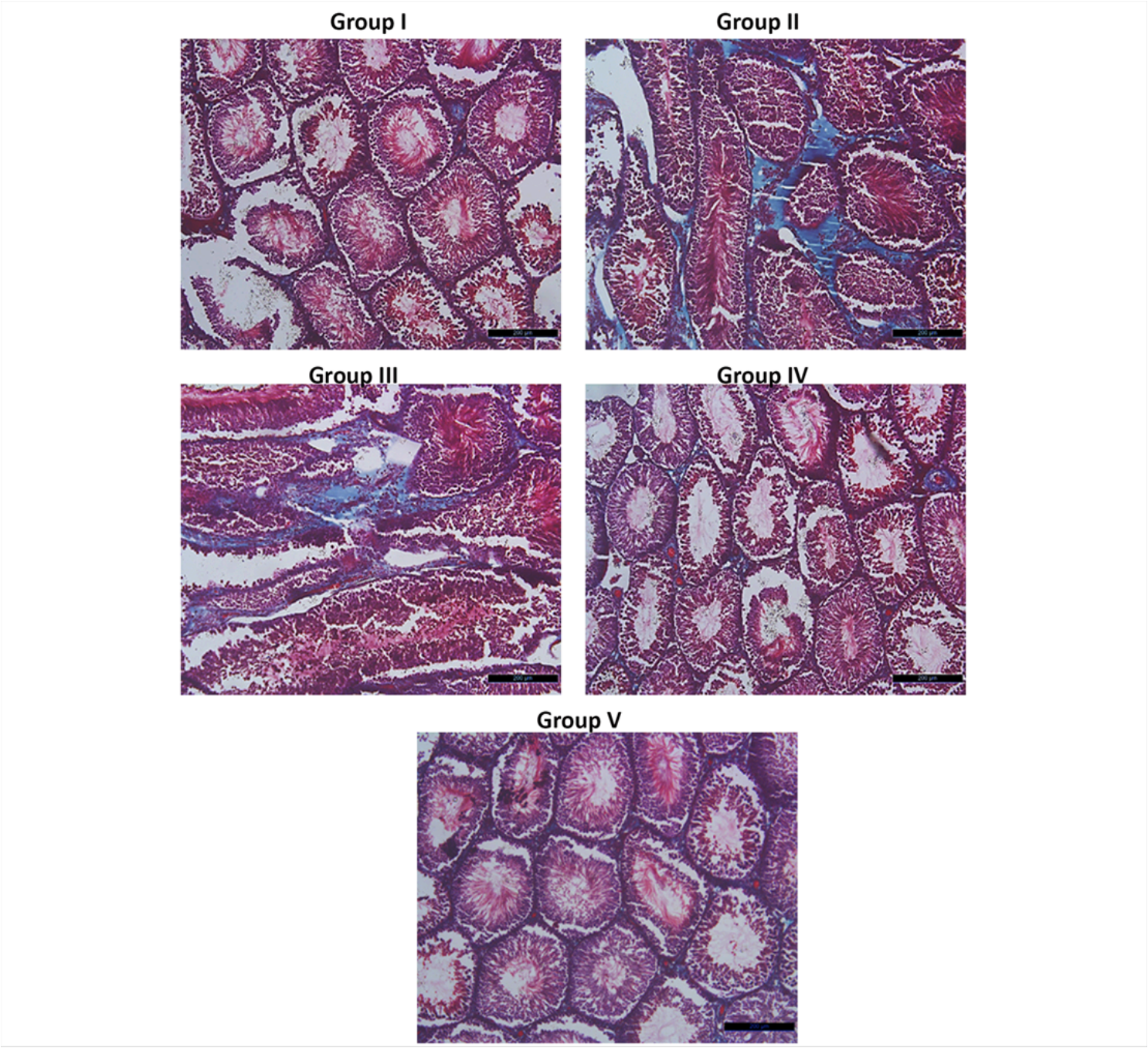

Figure 8

β-Caryophyllene reduces paclitaxel-induced collagen deposition and fibrotic remodeling in testicular tissue. Group I: control, Group II: PTX, Group III: PTX+BCP (25mg/kg) Group IV: PTX+BCP (50mg/kg).Group V: BCP alone. Representative photomicrographs of Masson trichrome stained testicular sections (×20 magnification).

Supplementary Files

This is a list of supplementary files associated with this preprint. Click to download.

- AuthorChecklistFull.pdf
- UncroppedWB.pdf
- Graphicalabstract.png